# MIXTURES OF FINE-GRAINED MINERALS –
# KAOLINITE AND CARBONATE GRAINS

Angelica M. Palomino[1,*], Susan E. Burns[2], and J. Carlos Santamarina[2]

[1] School of Civil and Environmental Engineering, Pennsylvania State University, 226A Sackett Building, University Park, Pennsylvania 16802, USA
[2] School of Civil and Environmental Engineering, Georgia Institute of Technology, 790 Atlantic Drive, Atlanta, Georgia 30332-0355, USA

**Abstract**—The behavior of mineral mixtures can be significantly different from the behavior of the individual components of the mixture due to differences between the mechanical and chemical properties of the individual minerals, and their ensuing effects on interparticle interactions and fabric formation. This study examines mixtures of kaolinite and calcium carbonate at different mass fractions using sedimentation, viscosity, and liquid-limit tests. These macroscale tests represent a wide range of solid-volume fractions and strain levels, with emphasis on high water-content conditions to magnify the effects of electrical forces. The results demonstrate that interparticle interactions depend on mineral surface-fluid effects, particle geometry, relative particle size, and solids content. With small solids contents, the kaolinite/calcium carbonate mixture behavior is a function of electrostatic interactions between oppositely charged mineral particles that promote flocculation; however, with large solids contents, the specific surface area of the minerals is the controlling factor. These results are relevant to many natural soil environments and to the possible development of engineered mineral mixtures for industrial applications.

**Key Words**—Calcium Carbonate, Fabric, Kaolinite, Liquid Limit, Sedimentation, Viscosity.

## INTRODUCTION

Particle mixtures often exhibit behavior not present in the individual components and deviate from values predicted by simple mass-average interpolations. Emergent phenomena depend on the grain size of the mixture components. The behavior of coarse-grained soil mixtures (of which the diameter of only 50% of the material ($d_{50}$) is finer than ~50 μm) is determined by geometric and mechanical characteristics. For example, mixtures of small and large grains can improve packing efficiency to attain high density (Furnas, 1931; Carman, 1937; White and Walton, 1937; German, 1989), while mixtures of rounded sand and platy mica grains have a more open fabric, are less stiff, and have a smaller critical-state friction angle than the sand without mica (Guimaraes, 2002).

Mixtures of fine and coarse grains exhibit unique behavior, often related to phenomena such as the formation of a coarse-grained granular skeleton (large mass fraction of coarse particles), the percolation of large open pores (small mass fraction of small particles), or mixing induced by rotating coarse grains during shear (Leelanitkul, 1989; Vipulanandan and Leung, 1991; Marion *et al.*, 1992; Bradford and Blanchar, 1999).

This study explores the behavior of mixtures made of fine-grained minerals ($d_{50} < $~20 μm). In this case, fabric

formation and response are controlled by electrostatic interactions in addition to geometric characteristics, and are often influenced by the pore fluid and the nature of the minerals. For example, the plasticity or viscosity of kaolinite-montmorillonite or illite-montmorillonite mixtures is not a linear function of the mass fraction of montmorillonite or the specific surface of the mixture (Keren, 1989; Mitchell, 1993; Ahmad *et al.*, 2000).

The study was designed to gain further insight into the short-term behavior of mixtures of fine-grained minerals, taking into consideration both geometric and electrostatic interactions. In particular, mixtures of kaolinite and calcium carbonate were investigated because of their different surface-charge characteristics as a function of pH. Tests were selected that provide short-term information related to fabric formation and granular interactions, by means of sedimentation tests, rheological/viscosity tests, and liquid-limit measurements. These large-water-content tests were selected to minimize the effects of particle collisions and to identify the onset of concentration-dependent processes.

## EXPERIMENTAL DESIGN

### Materials

Three kaolinites and two calcium carbonates were selected for this study. Scanning electron micrographs (SEM) of the materials were obtained using an Hitachi S100 SEM (Figure 1). The material characteristics and parameters vary with type (Table 1). Two kaolinite samples (Wilklay SA1 and Wilklay RP2) were obtained from Wilkinson Kaolin Associates (Gordon, Georgia,

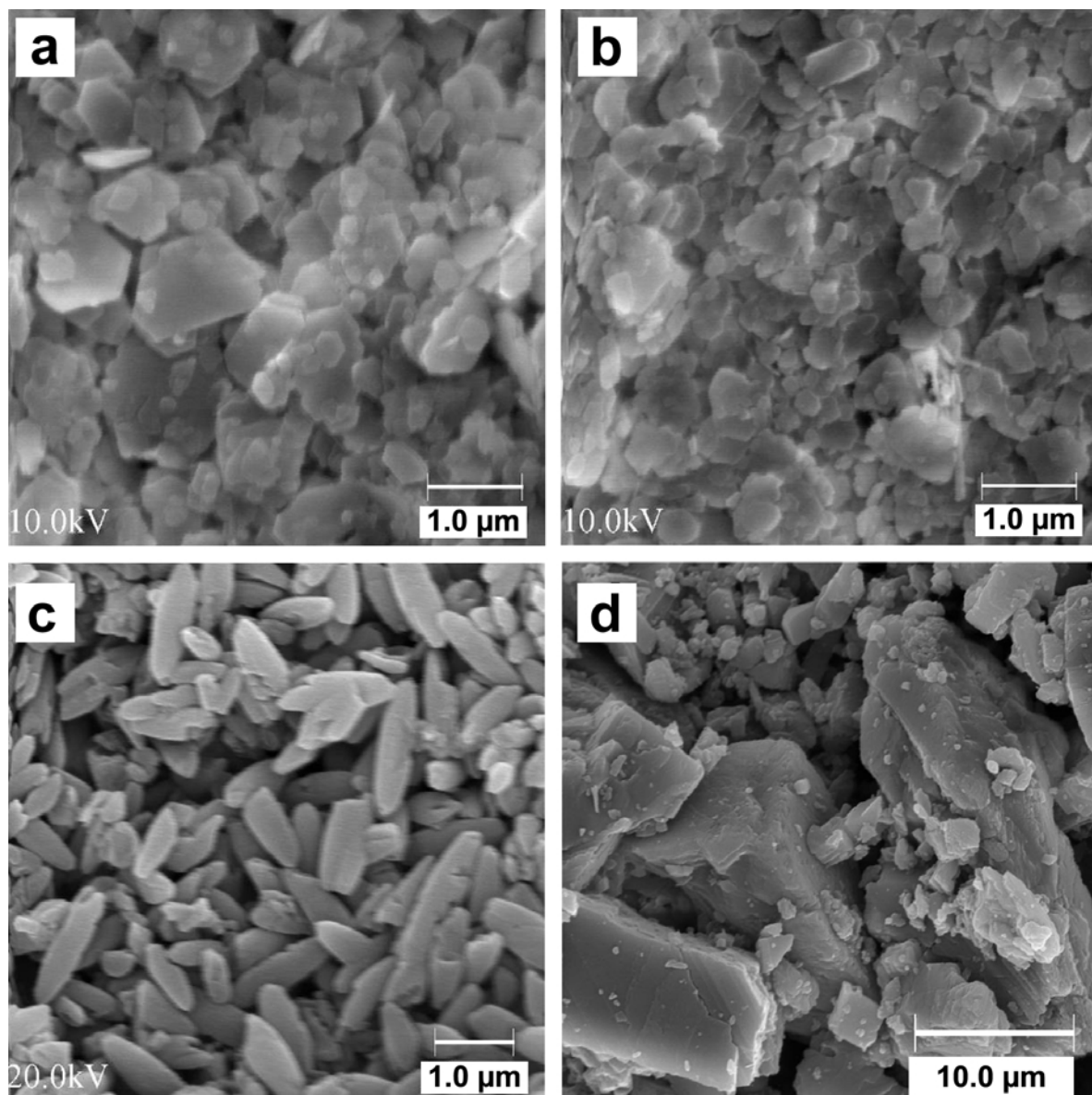* E-mail address of corresponding author:
amp26@psu.edu

Figure 1. SEM images of test materials: (a) kaolinite SA1; (b) kaolinite RP2; (c) PCC rhombic; and (d) GCC #12 White with part d shown at a smaller scale.
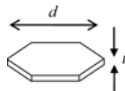
USA). Wilklay SA1 and RP2 are processed by air flotation with no chemical processing. The RP2 particles are smaller and thinner than the SA1 particles, with a greater specific surface area. The chemical analysis data of Wilklay RP2 and SA1 were provided by the manufacturer (Table 2). Note that the chemical analysis reveals only slight differences between the two materials.

In addition, a commercially available, surface-modified kaolinite, Premier (from Georgia, USA, supplied by IMERYS) was used to explore the potential modification of mineral mixtures through changes in surface chemistry and pore-fluid conditions. This clay resembles the SA1 clay in size, but was treated with a sodium

polyacrylate dispersant (NaPAA). This is an anionic polymer which electrostatically stabilizes kaolinite by binding to positive surface sites typically found on the particle edges. Any exposed negative sites along the polymer chain have the ability to bind to other positive sites such as the exposed surface Ca sites on non-surface-modified calcium carbonate particles.

The precipitated calcium carbonate (PCC) was obtained from Imerys and is a high-purity commercial product synthesized through the chemical reaction of $CaO$, $H_2O$, and $CO_2$. The reaction produces high-purity $CaCO_3$ crystals, the size and shape of which depend on the specific reaction process by controlling both the

Table 1. Characteristics of the tested materials.

| Material | Manufacturer | Surface state | Specific gravity[1] | pH[2] in deionized water | Conductivity[2] $\sigma$ ($\mu$S/cm) | Liquid limit[3] | Particle dimensions[4] | |
|---|---|---|---|---|---|---|---|---|
| Kaolinite SA1 | Wilkinson Kaolin Associates | Unmodified | 2.6 | 6.50 | 16.38 | 43 | | $d_{50}$ = 1.1 $\mu$m $t \approx$ 70 nm $S_a$ = 13.0 m²/g |
| Kaolinite RP2 | | Unmodified | 2.6 | 4.66 | 11.98 | 78 | | $d_{50}$ = 0.36 $\mu$m $t \approx$ 45 nm $S_a$ = 21.9 m²/g |
| Kaolinite Premier | Imerys, Pigments and Additives Group | Modified with NaPAA | 2.6 | 6.39 | 323 | – | | $d_{50} \approx$ 1 $\mu$m $t \approx$ 100 nm $S_a$ = 20.0 m²/g |
| PCC rhombic | | Unmodified | 2.71 | 9.87 | 101.90 | 52 | | $d_{50}$ = 1 $\mu$m $t \approx$ 0.50 $\mu$m $S_a$ = 10.0 m²/g |
| GCC #12 White | Georgia Marble Company | Unmodified | 2.71 | 8.76 | 54.60 | 28 | (to be enlarged 12×) | $d_{50}$ =12 $\mu$m $t \approx$ 12 $\mu$m $S_a$ = 1.98 m²/g |

[1] Manufacturer data; [2] measurements (resolution ±0.01 pH) of supernatant made at volumetric solids content $\phi$ = 0.02 in de-ionized water after centrifuging the suspensions; [3] measured using the fall-cone device (BS 1377); [4] the $d_{50}$ values are manufacturer data, particle thicknesses were measured from the SEM images, and the specific surface area measurements were obtained using gas adsorption by Klein (1999; SA1 and RP2) and M.C. Herrera (PCC and GCC). $d_{50}$ was obtained by sedimentation testing, which is a function of particle size and shape, and results in an equivalent grain size; therefore, $d_{50}$ is not directly comparable to $d$, the major dimension of the kaolinite particle. Note: GCC contains some trace impurities (1−5% $MgCO_3$) and acid insolubles (<3%) that may affect the pH value. The GCC particle is depicted as 1/12th of the actual relative size.

temperature and pressure, *i.e.* without crystal-habit modifiers (Imerys, 2003). The PCC product used for this study was obtained in dry powder form without surface additives. The scalenohedral particles are acicular, with an approximate length to diameter ratio of 2:1. The ground calcium carbonate (GCC) was obtained from Georgia Marble Company (Tate, Georgia, USA) and was produced by crushing and dry milling, without additives, naturally occurring limestone. As a consequence, GCC contains some trace impurities (1−5% $MgCO_3$ and <3% acid insolubles). Note that GCC is at least 10 times larger than the kaolinite particles.

Table 2. Chemical analysis (wt.%) of Wilklay RP2 and SA1 kaolin clays − manufacturer data.

| Chemical component | RP2 | SA1 |
|---|---|---|
| $SiO_2$ | 45.60 | 45.60 |
| $Al_2O_3$ | 38.40 | 38.40 |
| $Fe_2O_3$ | 0.88 | 0.40 |
| $TiO_2$ | 1.69 | 1.50 |
| CaO | 0.05 | 0.06 |
| MgO | 0.02 | Trace |
| $K_2O$ | 0.15 | 0.18 |
| $Na_2O$ | 0.21 | Trace |
| LOI | 13.70 | 13.82 |

*Experimental methods*

*Sedimentation*. A 2.54 cm-diameter acrylic cylinder was first filled with ~10 mL of deionized water. The solids were mixed gently with the fluid in the cylinder before additional fluid was poured into the cylinder to reach a total height of 17.0 cm, corresponding to 86.1 mL and a solids content (volume solids/total volume) of 0.02. The suspensions were mixed slowly with a perforated plunger until a uniform appearance was observed. The suspensions equilibrated overnight allowing time for the surfaces of the particles to adsorb water, ions, and/or polymer molecules and for the system to reach a stable pH. The suspensions were then remixed. Entrapped air was removed with a low vacuum, −15 kPa. Once the air had been evacuated (no evidence of bubble formation), and without releasing the vacuum, each cylinder was inverted repeatedly for ~1 min. After the last inversion, the cylinder was placed on a level surface. This point was defined as time zero. The vacuum was removed and the cylinder was capped with a rubber stopper. Both the suspension and sediment heights were monitored with time. The heights were recorded starting at $t$ = 15 s, and each subsequent reading was taken at twice the time interval of the previous reading, *i.e.* $t_1$ = 15 s, $t_2$ = 30 s, $t_3$ = 1 min, *etc*. The supernatant pH of each suspension was measured using an Accumet AR50 pH meter with a resolution of 0.01 pH (Fisher Scientific).

*Viscosity*. Viscosity was measured as follows. 400-mL suspensions were prepared in a 600-mL beaker. The beaker was placed on a Corning magnetic stirrer and mixed for at least 8 h prior to measurement. The suspension viscosities were measured using a Brookfield DV-E Viscometer fitted with spindle #1 (56.26 mm) for lower-viscosity suspensions or #2 (46.93 mm) for higher-viscosity suspensions, depending on the slurry consistency. The spindle rotation speed was varied between 1 and 100 rpm, and the viscosity reading was recorded after 1.5 min for every rotation speed setting. Between readings, the suspensions were mixed well for ~20 s to counteract any particle settlement.

*Liquid limit*. The shear strength near the liquid limit (LL) was determined as specified by British Standard 1377 (British Standard, 1990). The liquid limit is the water content at which an 80 g stainless steel cone with a 30° angle penetrates a remolded 20 mm soil specimen, when the cone is released at the soil surface. Penetration measurements were taken using a Wykeham Farrance cone penetrometer at four moisture levels for each remolded mineral mixture, and the cone penetration depths were plotted *vs.* the percentage moisture contents.

Viscosity, sedimentation, and liquid-limit tests were performed with single minerals: SA1, RP2, Premier, PCC, and GCC, and for mixtures of minerals: SA1:PCC, SA1:GCC, RP2:GCC, and Premier:PCC.

## RESULTS

Kaolinite, calcium carbonate, and kaolinite-calcium carbonate mixtures were evaluated using sedimentation, viscosity, and liquid-limit tests, which represent a broad range of mass fractions, strain rates, and strain levels (details and the complete data set can be found in Palomino, 2004).

### Single-mineral studies

*Sedimentation*. Three sedimentation characteristics were used to infer the suspension state of dispersion (see schematic of a typical sedimentation curve presented in Figure 2 insert): induction period; initial settlement velocity, $\alpha$; and final sediment height, $H$. The initial settlement velocity, $\alpha$, is the slope of the settlement-time curve during the induction period. The induction period is the initial portion of the settlement-time curve prior to the 'break' in the sedimentation curve, and $\alpha$ is calculated based on a linear-linear scale. During the induction period, the initial suspension consists of interconnected flow units with highly tortuous fluid-flow paths between them, and hindered fluid displacement. As time progresses, the flow units tend to line up, shortening the flow paths between them and allowing settlement to take place (Michaels and Bolger, 1962). The induction period and the initial settlement velocity, $\alpha$, are measures of the degree of particle associations just before the particles, flocs, or aggregates (all referred to as flow units) begin to settle (Tiller and Khatib, 1984; Palomino and Santamarina, 2005); therefore, the induction period is relatively long for dispersed systems. In dispersed systems, individual units, whether aggregates or single particles, segregate according to size during sedimentation. Yet, these units will settle in a minimum-energy configuration such that the resulting sediment is more compact compared to a flocculated system. Final sediment heights, $H$, tend to increase as flocculation increases, especially for edge-to-face (EF) flocculated systems; this situation prevails at small ionic concentrations near the isoelectric point, in the absence of surface modifiers.

Sedimentation signatures (Figure 2) for SA1 kaolinite and the treated Premier kaolinite have much longer induction periods and very slow settlement velocities compared to the RP2 kaolinite and to both carbonates,
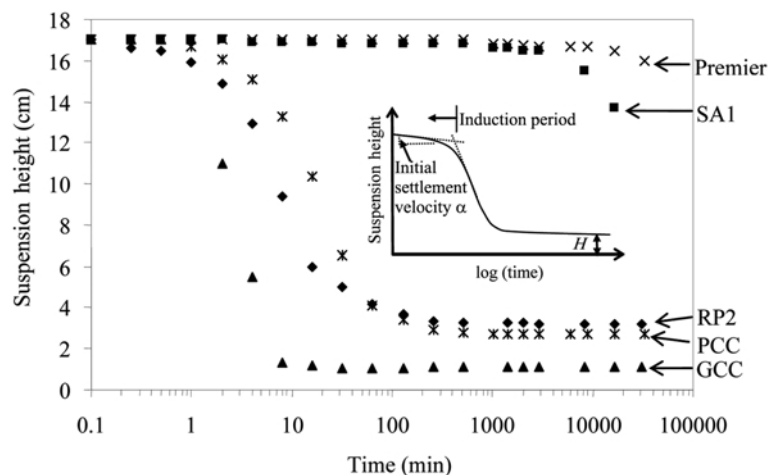


Figure 2. Sedimentation test. Signatures for the selected single-mineral grains. Characteristic parameters include the initial sedimentation velocity, the induction time, and the final suspension height, $H$ (shown in the insert). The suspension heights were determined at the water-suspension interface.
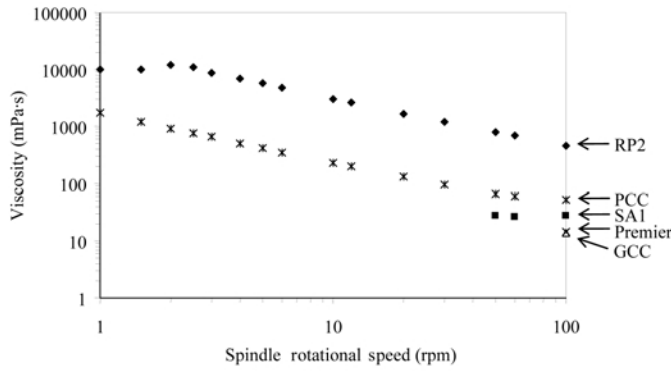
Figure 3. Viscosity test. Signatures for the selected single-mineral grains. A negative slope is the characteristic response of a shear-thinning suspension.

indicating that Premier and SA1 particles were more dispersed than the other minerals.

*Viscosity*. Viscosity-test signatures for selected single-mineral grains (Figure 3) reveal that the dispersed SA1 and Premier kaolinite suspensions yielded relatively small viscosity values compared to the flocculated RP2 suspension. Note that the viscosities of the SA1, Premier, and GCC suspensions were below the detection limit of the viscometer at low rpm values. The RP2 and PCC suspensions exhibited clear shear-thinning behavior, *i.e.* decreasing viscosity with increasing shear rate. Shear thinning is associated with reductions in the number of interparticle bonds and in the size of flow units with increasing shear rate in a flocculated suspension (Michaels and Bolger, 1964; Nicol and Hunter, 1970; Rand and Melton, 1977; Van Olphen, 1977; Hunter, 2001). Shear thinning also reflects particle alignment and reduction in flow resistance; this may be the prevailing effect for this acicular PCC.

*Liquid limit*. The liquid limit is the gravimetric water content at the boundary between plastic and liquid states of a large solids-volume fraction mixture. The shear strength at the liquid limit varies between 1.3 and 2.4 kPa (Wroth and Wood, 1978). Modifying the pore-fluid (fluid between the particles) chemistry will alter fabric, the resistance of the sol to shear, and in turn the liquid limit (Mitchell, 1993). Fall-cone test signatures for selected mineral grains (Figure 4) show that the more dispersed SA1 kaolinite exhibited a smaller liquid limit value than the RP2 kaolinite. The sensitivity to water content is denoted by the slope of the measured shear resistance (cone penetration depth) *vs*. water content: the greater the slope, the more rapidly the shear strength of the sol decreases for a given increase in water content or decrease in solids fraction. For example, the shear strength of the SA1 kaolinite (dispersed) has a much greater sensitivity to water content than the RP2 kaolinite (non-dispersed).

## KAOLINITE-CALCIUM CARBONATE MIXTURES

Tests were performed on mixtures of kaolinite, calcium carbonate, and surface-modified Premier kaolinite to assess physicochemical effects including pH, geometry, and ionic concentration. Note that mineral segregation was not observed in any of the mixture studies presented here.
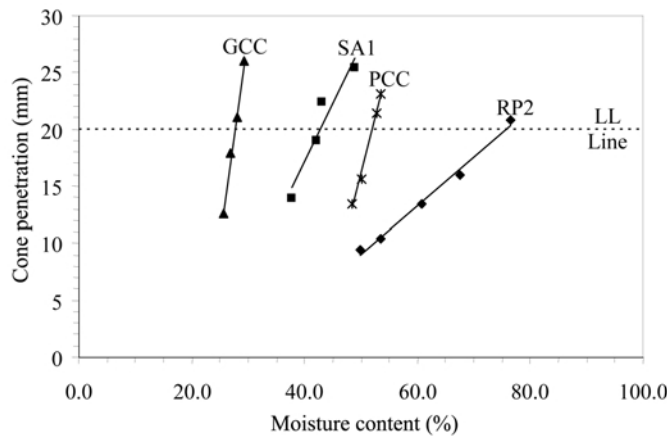


Figure 4. Cone penetration test and liquid limit − signatures for the selected single-mineral grains.

*Impact of differing mineral surface chemistry*

*Viscosity*. The impact of $CaCO_3$ on pore-fluid pH has direct consequences for mineral mixture behavior, which is evident through the rheological and plastic response of kaolinite-carbonate mixtures. The viscosity profiles of SA1:PCC mixtures as a function of spindle rotation speed reveal the shear thinning behavior of each suspension (Figure 5a). Particle interaction reaches a maximum near the 25% SA1 mixture when comparing the measured viscosity at 100 rpm for the SA1:PCC systems (Figure 5b).

*Liquid limit*. Fall-cone penetration lines for the given SA1:GCC mineral mixtures (Figure 6a) were used to determine the liquid limit and the slopes of the liquid-limit lines for the tested mixtures (Figure 6b). Both the minimum liquid limit and maximum slope (Figure 6b) occur at 20% kaolinite, *i.e.* away from the endpoints (100% kaolinite or 100% $CaCO_3$), highlighting the relevance of particle-level interactions over total specific surface for this mixture. For greater mass fractions of kaolinite, the increasing liquid limit with decreasing slope (also observed for single minerals by Palomino and Santamarina, 2005) indicates that plasticity increases and the sensitivity to water content decreases as the surface area increases.

Previous studies of kaolinite-carbonate mixtures have shown similar trends to those seen in this study. Hagemeyer (1960) showed that sediment volume of mixtures of platy kaolinite and needle-shaped $CaCO_3$ (similar to the PCC used here) reaches a maximum at 30% kaolinite mass fraction. The liquid limits of mixtures of untreated chalk and kaolinite tested by Arkin and Michaeli (1989) fall in the same range as those mixtures presented here.

*Sedimentation and grain geometry (size and shape)*

The initial settlement velocities for RP2-GCC and SA1-GCC mixtures at various mass fractions of clay were compared (Figure 7). The settling velocity for the SA1-GCC mixtures was very small and independent of mass fraction of clay, *i.e.* all these mixtures exhibited very short induction times. In contrast, the RP2-GCC mixtures had settling velocities indicative of flocculated suspensions; the settling velocity varied with clay mass fraction and has an apparent peak at 10% RP2.

The effects of relative geometry on the RP2-GCC and SA1-GCC sediment heights were investigated (Figure 8), with sediment height measured when no visible particles remained in suspension. While the GCC mean particle diameter was >10 times greater than either clay particle size, the results show increasing sediment
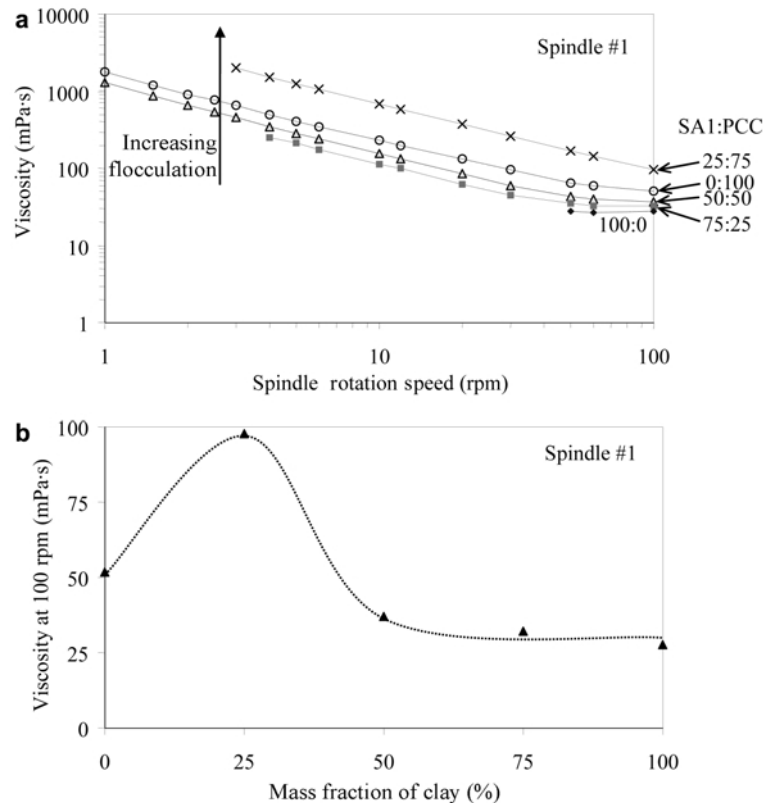


Figure 5. Viscosity of the SA1 and PCC mixtures: (a) typical trends for viscosity as a function of spindle rotation speeds; (b) viscosity as a function of the mass fraction of clay (at a spindle rotation speed of 100 rpm).
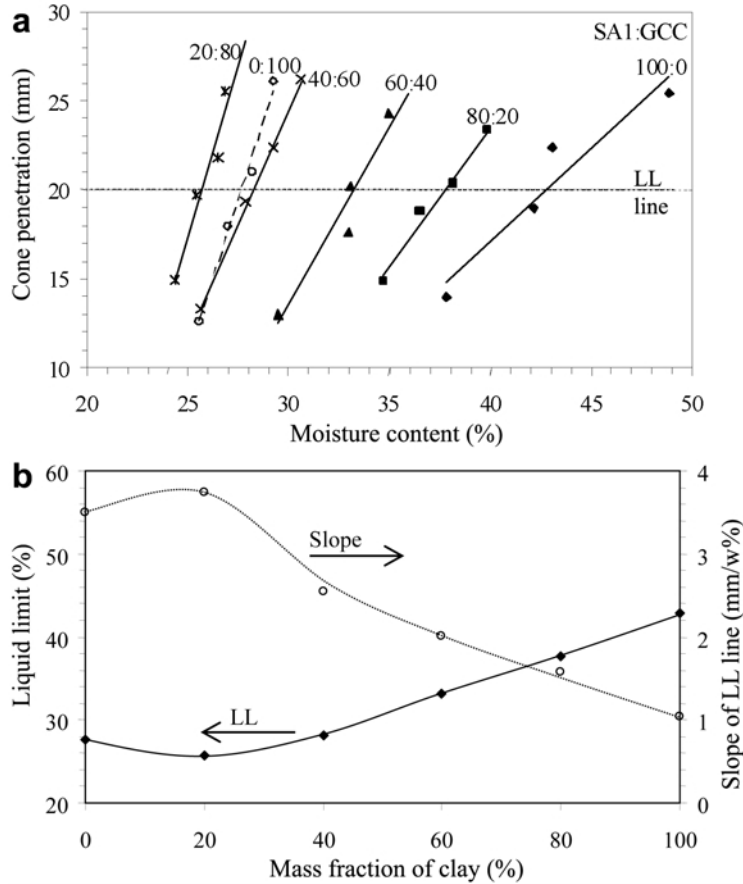
Figure 6. Plasticity of the SA1 and GCC mixtures: (a) fall-cone penetration lines; (b) liquid limits (LL) and sensitivity to moisture content as a function of clay fraction.

height with increasing clay mass fraction even at small clay contents (this would not be the case in coarse-grained mixtures). The decrease and relatively small sediment height for the 100% SA1 kaolinite suspension is consistent with the dispersive tendency of the clay at its self-buffering pH (Table 1).

*Modification of surface chemistry and pore fluid*

Modification of interparticle interactions in fine-grained mixtures is also possible by altering the surface chemistry and/or the pore-fluid chemistry. Previous studies have explored kaolinite-carbonate-mixture behavior in the presence of dispersants in view of paper-
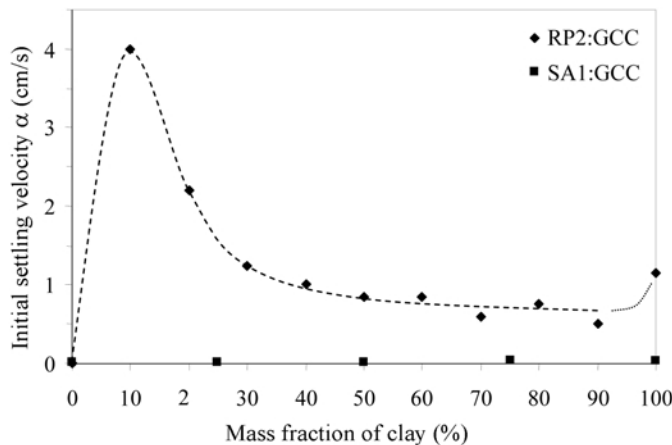


Figure 7. The effect of relative geometry on the initial settling velocity, $\alpha$, of dilute suspensions. The mixtures were prepared with the same carbonate GCC, but with different kaolinites: RP2, SA1.
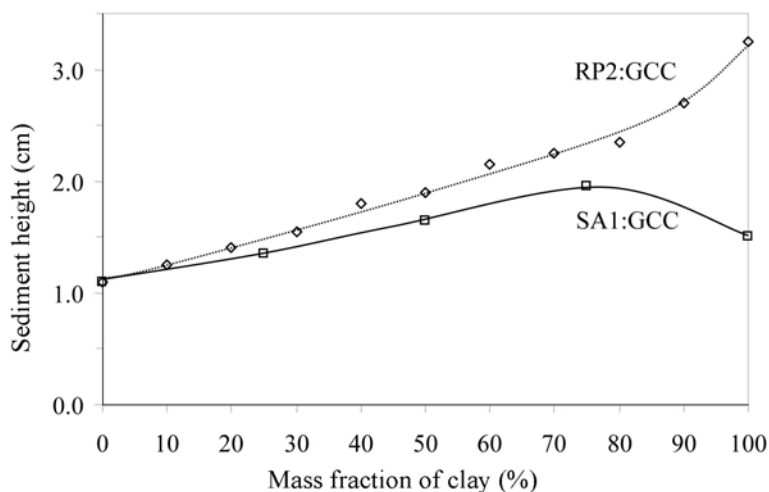
Figure 8. The effect of relative geometry on the 273 *H* sediment height of dilute suspensions. The mixtures were prepared with the same carbonate GCC, but with different kaolinites: RP2, SA1. The sediment height is determined at the sediment-suspension interface.

coating applications (Hagemeyer, 1960; Huber and Weigl, 1972; Dahlvik *et al.*, 1995). Both techniques are explored in this section using the NaPAA surface-treated Premier kaolinite and precipitated calcium carbonate PCC (the PCC particles have no surface additives, and both particles have similar characteristic dimensions, ~1 μm, Table 1). The sedimentation behavior of the Premier material was modified by various mass fractions of PCC (Figure 9). The suspension response ranged from dispersive, noted from the extended induction period for the 100% kaolinite case, to induced flocculation at greater mass fractions of PCC.

The impact of cations on the pore fluid of the Premier kaolinite-PCC particle mixture was assessed through the addition of $CaCl_2$. $Ca^{2+}$ ions are expected to bind to the polymer sites vacated by $Na^+$ along the polyacrylate chain, yielding an excess positive charge that promotes flocculation between polymer-coated kaolinite particles. The impact of enhanced flocculation tendency was evaluated through sedimentation, viscosity, and liquid limit tests, with and without $CaCl_2$; tests with $CaCl_2$ were made at the same concentration in the pore fluid ($c$ = 0.002 M $CaCl_2$). In the absence of $CaCl_2$, the maximum sediment height for the Premier:PCC mixture occurred for the 25% mass fraction of clay (Figure 10); however, this maximum sediment height was exceeded by the sediment heights of all mixtures containing $CaCl_2$, which reached an apparent peak at 75% mass fraction of clay. $CaCl_2$-induced flocculation was also observed in viscosity measurements (Figure 11); however, the viscosity peaks take place at 25% mass fraction of the clay. Finally, the liquid-limit values obtained for the series with and without $CaCl_2$ differ very little (Figure 12). The distinct effect of $CaCl_2$ in these tests reflects the decreasing ratio between the $Ca^{2+}$ added to the number of available binding sites on the polymer chains as the solids content increases from sedimentation to liquid-limit tests.
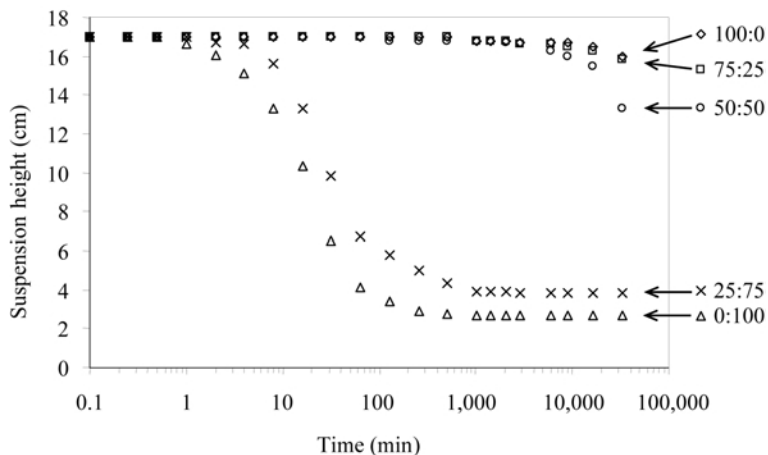


Figure 9. Controlling particle interaction through changes in surface chemistry: sedimentation curves for Premier-PCC mixtures.
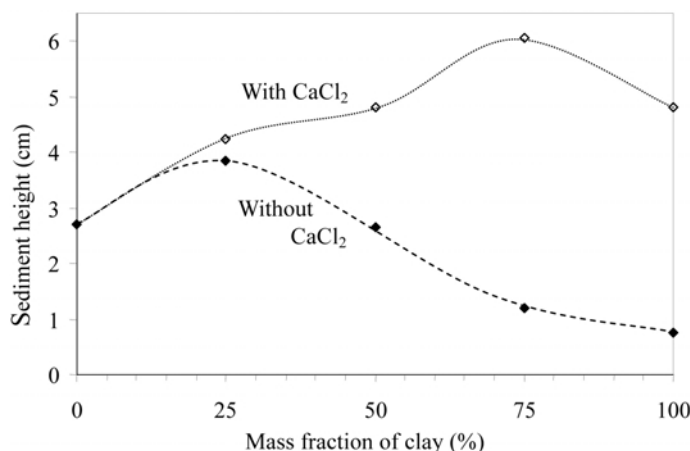
Figure 10. Controlling particle interaction through changes in surface chemistry and pore fluid. Final sediment height at 23 days for Premier-PCC mixtures with and without $CaCl_2$.

## DISCUSSION

### Pore-fluid effects

The fabric within fine-grained, single-mineral systems is determined primarily by the pore-fluid characteristics, *e.g.* pH and ionic concentration (Santamarina *et al.*, 2002). Coulombic forces can be enhanced or repressed to achieve flocculation or dispersion by altering the relative magnitude between them and the existing van der Waals forces. In contrast, controlling the fabric of mixtures of fine-grained minerals requires insight into both the mineral-surface chemistry and the particle geometry of each mineral type: *e.g.* (1) the fabric was opened when the platy kaolinite particles bridged the ellipsoidal carbonate particles at 25% mass fraction of clay; and (2) polymers and other modifiers can be added to the pore fluid to produce higher-order fabrics (Figures 10, 11).

The surface-charge characteristics of both kaolinite and calcium carbonate are functions of the pH of the pore fluid. The isoelectric point of kaolinite typically ranges between 4 and 6 (Sposito, 1989; Drever, 1997; Yuan and Pruett, 1998), while that of $CaCO_3$ is between 8 and 10.5 (Siffert and Fimbel, 1984). Consequently, at neutral pH conditions, kaolinite particle faces have a net negative charge, while $CaCO_3$ particles that have not been chemically modified have a net positive charge (Figure 13). Note that these properties are for the single minerals in deionized water and change when other species are present in the solution. Additionally, the zeta potential for both materials varies with pH; the zeta potential for kaolinite ranges from positive values at very low pH (~ +5 mV at pH 1.5) to negative values at moderate to high pH (up to ~ −50 mV at pH 10 (Yuan and Pruett, 1998)).

For suspensions containing only $CaCO_3$ (or $CaCO_3$ with trace $CaMg(CO_3)_2$) that are mixed with deionized water in equilibrium with atmospheric $CO_2$, the measured supernatant pH is ~8. Calcium carbonate dissolution occurs according to the following reaction:

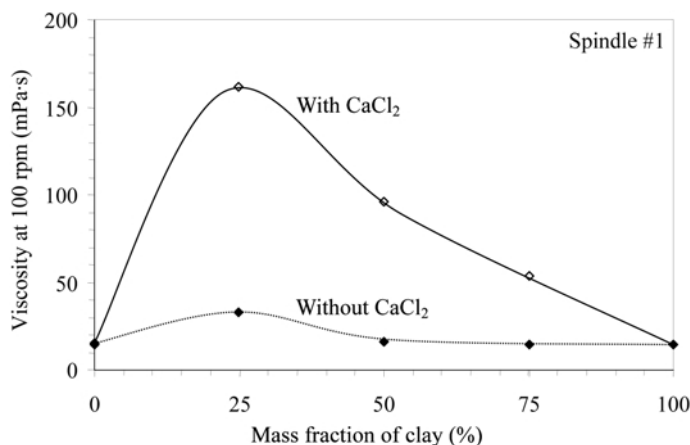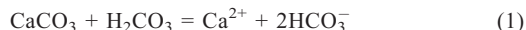$$CaCO_3 + H_2CO_3 = Ca^{2+} + 2HCO_3^- \qquad (1)$$



Figure 11. Controlling particle interaction through changes in surface chemistry and pore fluid. Viscosity at 100 rpm for Premier-PCC mixtures with and without $CaCl_2$.
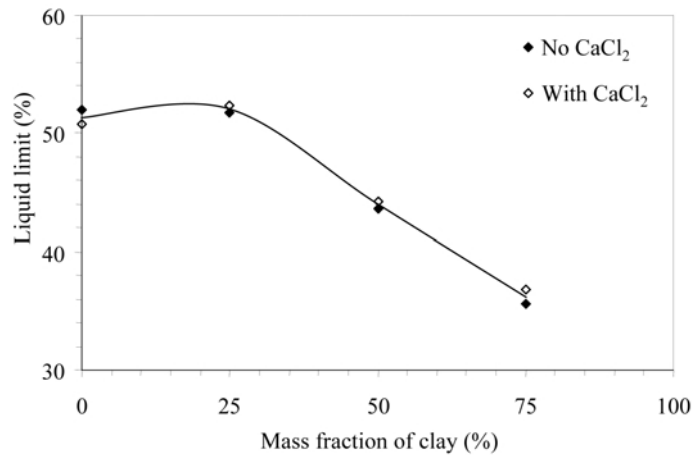
Figure 12. Controlling particle interaction through changes in surface chemistry and pore fluid. Liquid limit for Premier-PCC mixtures with and without CaCl$_2$.

The pH of these suspensions is controlled by the aqueous chemistry of carbonate, with bicarbonate (HCO$_3^-$) as the predominant form of carbonate at pH = 8.1.

In contrast, suspensions containing 100% kaolinite and deionized water in equilibrium with atmospheric CO$_2$ result in an equilibrium pH = 4.4. When only kaolinite is added to pure water in equilibrium with atmospheric CO$_2$, the mineral dissolves until an equilibrium pH is achieved. The dissolution of kaolinite in water is accompanied by the release of H$^+$ (acidification) and the formation of dissolved aluminum hydroxide species and orthosilicic acid (H$_4$SiO$_4$) and its dissociation products.

For suspensions that contain both CaCO$_3$ and kaolinite, the suspension pH was moderated by the buffer capacity of the carbonate with measured pH values between 7.6 and 7.9, even in suspensions that were as much as 90% kaolinite by weight (Figure 14, pH at 21 days). The different self-buffering pH of the individual minerals implies different surface charge, mutual attraction, and a greater degree of structure in the short term (Figures 7, 8). As in previous studies of mineral mixtures, the focus in the present study was also on short-term responses, such as those observed through sedimentation, viscosity, and liquid-limit tests (Hagemeyer, 1960; Huber and Weigl, 1972).
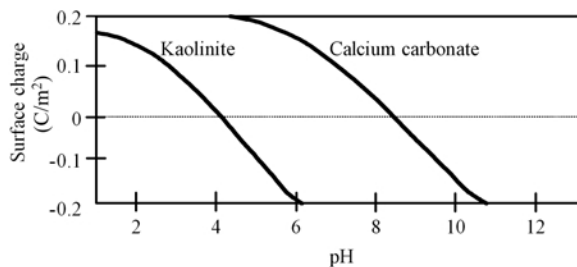
In the long term, the continuous dissolution of both components leads to the precipitation of new minerals. Geochemical modeling using the program PHREEQC (Parkhurst and Appelo, 1999) predicts that at equilibrium, gibbsite Al(OH)$_3$, which formed from the structural aluminum released during kaolinite dissolution, would precipitate in the kaolinite/carbonate suspension (its presence was not verified in the experiments). Clearly, the long-term behavior of a granular mixture is strongly dependent on its mineralogical makeup, which depends on the source material (parent rock), depositional environment, and post-depositional chemical reactions. While short-term observations yield the impression that soils are in equilibrium, most soils are continuously changing when observed during long periods; volcanic ash soils are a clear example (Herrera *et al.*, 2007). Water in soil pores facilitates these changes by allowing dissolution, leaching of some species, and precipitation of new minerals.

*Geometric effects*

Even in the case of fine grains, particle geometry makes an important contribution to overall behavior. For example, kaolinite particles have exposed edges that can



Figure 13. Effect of pH on the surface charge of kaolinite and calcium carbonate (data from Stumm *et al.*, 1992).
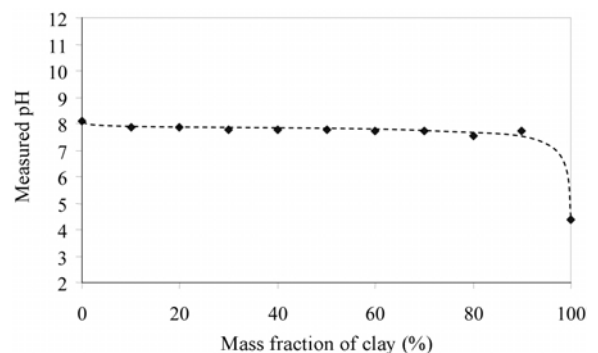


Figure 14. Supernatant pH of kaolinite and carbonate mixtures RP2:GCC at 21 days.

develop a net charge opposite to that of the particle face and lead to EF flocculation. However, for montmorillonite particles, the edge charge is shielded by the ionic cloud created by the particle face, and different fabrics are expected (Santamarina *et al.*, 2002).

Grain size dictates the relative contribution of gravimetric and electrical forces dominating the particle behavior, especially during sedimentation. Figure 15 illustrates probable particle interactions among single minerals and mineral mixtures for both coarse-grained and fine-grained materials. A coarse-grained particle fabric ($d_{50} > \sim 50$ μm) develops through gravimetric forces. Particle packings include stacked configurations for platy particles, such as mica flakes, and simple cubic and tetrahedral configurations for spherical particles. Mixtures of spherical particles with varying diameters form denser packings than single-diameter particles, while platy-spherical mixtures may form more open fabrics due to particle bridging (Lee *et al.*, 2007). In contrast to fine particles, additives designed to modify surface charge have little influence on coarse interparticle associations.

*Dispersed vs. non-dispersed systems*

The combination of changes in pore-fluid chemistry and differences in particle geometry contribute to the creation of more structured, or non-dispersed, systems from dispersed single-mineral systems. For example, combining SA1 (dispersed) kaolinite with GCC (dispersed) creates a more voluminous structure, seen as a larger sediment height, compared to either single-mineral case for the same solids content. (The pure phase, GCC, is considered to be dispersed because the individual particles do not form larger aggregates.) Even though the GCC particles are ~10 times larger than the SA1 particles (Table 1), the greater sediment height of the mixture indicates formation of clay-clay and/or clay-GCC flocs. The fluid pH of the GCC-containing suspensions renders the clay particles with net negatively charged faces and edges, so that clay-clay flocs are less likely to form. Yet, dissolution of GCC releases $Ca^{2+}$ ions that may adsorb onto the clay mineral surface, alter the net surface charge, and promote edge-to-face flocculation under small-solids-content conditions.

Mixtures of dispersed and non-dispersed minerals are more likely to result in non-dispersed systems. Mixtures of SA1:PCC (dispersed:non-dispersed) and RP2:GCC (non-dispersed:dispersed) had characteristics of non-dispersed systems at small- and moderate-solids content, as shown by shear-thinning behavior (Figure 5a) and greater sediment heights (Figure 7). For the mixtures containing PCC, increasing particle alignment with increasing spindle rotation speed (Figure 5a) contributed to the shear-thinning response of the suspension. Note that in the case of RP2:GCC, the sediment heights are more voluminous, *i.e.* more flocculated, than the
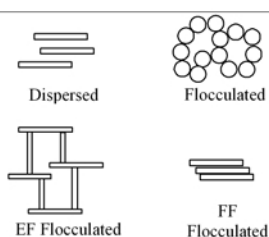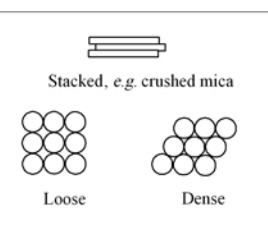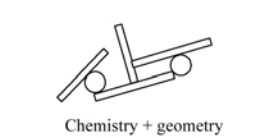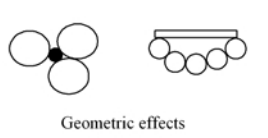


Figure 15. Mixtures in coarse- and fine-grained soils. Probable particle associations in single-mineral and mineral-mixture systems.

SA1:GCC mixtures even though the size of the RP2 particles are approximately one-third that of the SA1 particles.

The surface-treated Premier kaolinite (dispersed), when mixed with PCC (non-dispersed), forms non-dispersed systems. Structure formation was enhanced overall with the addition of $CaCl_2$ due to both the geometry of the PCC particles and the presence of $Ca^{2+}$ ions.

## CONCLUSIONS

The behavior of fine-grained mineral mixtures is due in part to interparticle electrical forces. These forces are determined by the surrounding pore-fluid pH, which is itself determined by the minerals present in their non-surface-modified state.

Mixtures of kaolinite and calcium carbonate grains exhibited behavior that is related to the pH-dependent mineral-surface charge, the relative size and shapes of the particles, and their mass fraction.

The presence of carbonate controlled the pH of mixtures even when the clay mass fraction reached 90%.

Particle flocculation took place due to electrostatic interactions between the positively charged calcium carbonate and the negatively charged kaolinite particles at carbonate-controlled pH conditions.

Mixtures of dispersed and non-dispersed phases were more likely to result in non-dispersed, *i.e.* flocculated, systems, at least at small and moderate solid contents.

Both sedimentation and the rheological behavior of dispersed:non-dispersed systems were consistent with systems that have particle associations.

The fabric was 'opened' when large platy clay particles bridge rounded or ellipsoidal carbonate particles (round cross-section); a high-porosity fabric can be achieved with small percentages of carbonate.

Grain mixtures made of different minerals bring about new phenomena, including short-term effects such as new fabrics (combined geometric and electrostatic effects), and longer-term effects associated with the dissolution of the two input minerals and the formation of new precipitates. This investigation addressed short-term effects.

The dependence of sedimentation and viscosity on particle associations gave way to specific surface in large-solids-content tests, such as the liquid limit.

Mixtures exhibited an extremum between 15 and 25% clay fraction: the greatest initial settling velocity, the greatest viscosity, and smallest liquid limit. This appears to be the limit between negatively charged kaolinite particles coating positively charged carbonate particles, and large-specific-surface-area kaolinite particles controlling overall behavior.

The behavior of fine-grained mixtures can be modified effectively and controlled by altering the surface chemistry of minerals and salt type and concentration in the pore fluid.

## REFERENCES

Ahmad, N.S., Karunaratne, G.P., Chew, S.H., and Lee, S.L. (2000) Bentonite-kaolinite mix for barrier systems. Pp. 93−104 in: *Geo-Denver 2000* (T.F. Zimmie, editor). ASCE, Denver, Colorado, USA.

Arkin, Y. and Michaeli, L. (1989) Strength and consistency of artificial clay-carbonate mixtures: Simulation of natural sediments. *Engineering Geology*, **26**, 201−213.

Bradford, J.M. and Blanchar, R.W. (1999) Mineralogy and water quality parameters in rill erosion of clay-sand mixtures. *Soil Science Society of America Journal*, **63**, 1300−1307.

British Standard (1990) Determination of liquid limit. **1377−90 Section 4**.

Carman, P.C. (1937) Fluid flow through granular beds. *Transactions of the Institution of Chemical Engineers*, **15**, 150−166.

Dahlvik, P., Ström, G., and Salminen, P. (1995) Effect of ph and calcium ion concentration on the flow behaviour and structure formation of clay/calcium carbonate suspensions. Pp. 63−69 in: *1995 Coating Fundamental Symposium*. TAPPI Proceedings, Technical Association of the Pulp and Paper Industries, South Norcross, Georgia, USA.

Drever, J.I. (1997) *The Geochemistry of Natural Waters: Surface and Groundwater Environments*. Prentice Hall, Upper Saddle River, New Jersey, USA.

Furnas, C.C. (1931) Grading aggregates I: Mathematical relations for beds for broken solids for maximum density. *Industrial Engineering Chemistry*, **23**, 1052−1058.

German, R.M. (1989) *Particle Packing Characteristics*. Metal Powder Industries Federation, Princeton, New Jersey, USA.

Guimaraes, M. (2002) Crushed stone fines and ion removal from clay slurries-fundamental studies. PhD dissertation, Georgia Institute of Technology, Atlanta, Georgia, USA, 238 pp.

Hagemeyer, R.W. (1960) The effect of pigment combination and solids concentration on particle packing and coated paper characteristics: I. Relationship of particle shape to particle packing. *TAPPI*, **43**, 277 − 288.

Herrera, M.C., Lizcano, A., and Santamarina, J.C. (2007) Colombian volcanic ash soils. Pp. 2385−2409 in: *Proceedings of the 2ⁿᵈ International Workshop on Characterization and Engineering Properties of Natural Soils* (T.S. Tan, K.K. Phoon, D.W. Hight, and S. Leroueil, editors). Taylor & Francis, The Netherlands.

Huber, O. and Weigl, J. (1972) Die füllstoff- und pigmentqualitä und ihr einfluß auf das papier. *Papier*, **26**, 545−554.

Hunter, R.J. (2001) *Foundations of Colloid Science*. Oxford University Press, Oxford, New York.

IMERYS (2003) *Products − pcc imerys worldwide paper division*. Retrieved May 28, 2003, from www.imerys-paper.com/html/pcc.html.

Keren, R. (1989) Rheology of mixed kaolinite-montmorillonite suspensions. *Soil Science Society of America Journal*, **53**, 725 − 730.

Lee, J.S., Guimaraes, M., and Santamarina, J.C. (2007) Micaceous sands: Microscale mechanisms and macroscale response. *Journal of Geotechnical and Geoenvironmental Engineering*, **133**, 1136−1143.

Leelanitkul, S. (1989) Improving properties of active clay by sand admixtures. Pp. 381−391 in: *Foundation Engineering*

*and Current Principles and Practices* (F.H. Kulhawy, editor). American Society of Chemical Engineers, New York.

Marion, D., Nur, A., Yin, H., and Han, D. (1992) Compressional velocity and porosity in sand-clay mixtures. *Geophysics*, **57**, 554−563.

Michaels, A.S. and Bolger, J.C. (1962) Settling rates and sediment volumes of flocculated kaolin suspensions. *Industrial and Engineering Chemistry Fundamentals*, **1**, 24−33.

Michaels, A.S. and Bolger, J.C. (1964) Particle interactions in aqueous kaolinite dispersions. *Industrial and Engineering Chemistry Fundamentals*, **3**, 14−20.

Mitchell, J.K. (1993) *Fundamentals of Soil Behavior*. John Wiley & Sons, New York.

Nicol, S.K. and Hunter, R.J. (1970) Some rheological and electrokinetic properties of kaolinite suspensions. *Australian Journal of Chemistry*, **23**, 2177−2186.

Palomino, A.M. (2004) Fabric formation and control in fine-grained materials. PhD dissertation, Georgia Institute of Technology, Atlanta, Georgia, USA, 193 pp.

Palomino, A.M. and Santamarina, J.C. (2005) Fabric map for kaolinite: Effects of pH and ionic concentration on behavior. *Clays and Clay Minerals*, **53**, 209−222.

Parkhurst, D.L. and Appelo, C.A.J. (1999) *Phreeqc* (version 2). A computer program for speciation, batch-reaction, one-dimensional transport, and inverse geochemical calculations. United States Geological Survey.

Rand, B. and Melton, I.E. (1977) Particle interactions in aqueous kaolinite suspensions I. Effect of pH and electrolyte upon the mode of particle interaction in homoionic sodium kaolinite suspensions. *Journal of Colloid and Interface Science*, **60**, 308−320.

Santamarina, J.C., Klein, K.A. Palomino, A., and Guimaraes, M.S. (2002) Micro-scale aspects of chemical-mechanical coupling: Interparticle forces and fabric. Pp. 47−64 in: *Chemo-mechanical Coupling in Clays: From nano-scale to Engineering Applications* (C.D. Maio, T. Hueckel and B. Loret, editors). A.A. Balkema, Lisse, The Netherlands.

Siffert, B. and Fimbel, P. (1984) Parameters affecting the sign and the magnitude of the electrokinetic potential of calcite. *Colloids and Surfaces*, **11**, 377−389.

Sposito, G. (1989) *The Chemistry of Soils*. Oxford University Press, New York.

Stumm, W., Sigg, L. and Sulzberger, B. (1992) *Chemistry of the solid-water interface: Processes at the mineral-water and particle-water interface in natural systems*. Wiley, New York.

Tiller, F.M. and Khatib, Z. (1984) The theory of sediment volumes of compressible, particulate structures. *Journal of Colloid and Interface Science*, **100**, 55−67.

Van Olphen, H. (1977) *An Introduction to Clay Colloid Chemistry: For Clay Technologists, Geologists, and Soil Scientists*. Wiley, New York.

Vipulanandan, C. and Leung, M. (1991) Effect of methanol and seepage control in permeable kaolinite soil. *Journal of Hazardous Materials*, **27**, 149−167.

White, H.E. and Walton, S.F. (1937) Particle packing and particle shape. *Journal of the American Ceramic Society*, **20**, 155−166.

Wroth, C.P. and Wood, D.M. (1978) The correlation of index properties with some basic engineering properties of soils. *Canadian Geotechnical Journal*, **15**, 137−145.

Yuan, J. and Pruett, R.J. (1998) Zeta potential and related properties of kaolin clays from Georgia. *Minerals and Metallurgical Processing*, **15**, 50−52.